Journal of Alloys and Compounds 509 (2011) 6589–6594

Contents lists available at ScienceDirect

Journal of Alloys and Compounds

journal homepage: www.elsevier.com/locate/jallcom

Modeling the swelling performance of UMo alloys for Al-matrix dispersion fuel☆

Liu Xiao[a,c,*], Lu Tie-cheng[a], Xing Zhong-hu[b], Qian Da-zhi[c]

[a] Physics Department of Sichuan University, Key Laboratory for Radiation Physics and Technology of the Education Ministry, Chengdu 610064, PR China
[b] Forth Sub-Institute, Nuclear Power Institute of China, Chengdu 610041, PR China
[c] Institute of Nuclear Physics and Chemistry, China Academy of Engineering Physics, Mianyang 621900, PR China

ARTICLE INFO

Article history:
Received 24 May 2010
Received in revised form 12 February 2011
Accepted 17 March 2011
Available online 29 March 2011

Key words:
UMo alloys
Grain subdivision
Swelling
Matrix creep

ABSTRACT

Fuel swelling by fission products is now considered the greatest factor that influences fuel performance. To gain a better understanding of the swelling behavior on UMo/Al fuel, we have investigated gas generation and have characterized fission-product swelling. The matrix-material creep and the interaction between the UMo fuel particles and the Al matrix have also been studied in the modeling of this process. The modeled phenomena also allow the prediction of UMo/Al fuel swelling. The results show that the motion of fission gaseous atoms, bubble growth and evolution and the creep of matrix materials are the basic behaviors of UMo/Al-dispersion fuel swelling. The swelling rate of the fuel exhibits a distinct knee. Before the grain subdivision, the degrees of fuel swelling at different fission rates are not evidently different. After the grain subdivision, the fuel swelling at lower fission rates is faster than that at higher fission rates. The matrix material experiences accelerated creep at high temperatures. If the fuel volume fraction is higher than 52%, the fuel swelling sharply increases after grain subdivision. The results are compared with the data from the literature, and these show reasonable agreement. The analysis provides a plausible interpretation of the behavior of UMo/Al-dispersion fuel swelling.

1. Introduction

UMo/Al-dispersion fuel has the advantages of having high density, excellent irradiation performance and good thermal conductivity, which are important to Reduced Enrichment for Research and Test Reactors (RERTR) and Research Reactor Fuel Management (RRFM). The goal of the RERTR program is to develop fuels for nuclear research and to test reactors that will facilitate the effective conversion of highly enriched uranium (HEU) fuel to low-enriched uranium (LEU) fuel, thereby reducing the threat of nuclear proliferation worldwide by minimizing the amount of HEU available to readily fabricate a nuclear weapon [1,2]. As uranium enrichment decreases, the uranium density in the fuel must increase to maintain the net fissile-atom density of the fuel. This requirement has driven efforts to develop high-uranium-density fuels that possess the greatest possible uranium density in the fuel region. UMo-dispersion fuel is one of the most advanced fuel candidates for the conversion of high-performance research reactors from HEU to LEU fuel, and significant effort has been directed toward its development and fabrication [3–9].

A number of irradiation experiments have been performed to determine the basic irradiation behavior of UMo fuel [10,11]. Early experiments have shown that metallic uranium alloys are excellent candidates for fuel materials [12,13]. However, past irradiation campaigns have shown that fuel consisting of UMo dispersed in a pure Al matrix cannot withstand severe irradiation conditions. UMo/Al-dispersion fuels form unacceptably large pores during irradiation due to the unstable properties of the interaction layer (IL) between the UMo fuel particle and the Al matrix. Some methods have been proposed to develop a modified UMo alloy that is capable of either forming a more stable IL or reducing its growth. One of these methods involves adding stabilizing elements to the UMo fuel and the Al matrix [14]. Development advances in UMo monolithic and dispersed fuels are presented to examine possible alternatives for HEU-LEU conversion [15].

The post-irradiation examination of these experimental fuels will provide the first glimpse into the irradiation performance of UMo/Al-dispersion fuels. The fuel type that appears most promising is envisioned. However, to gain a better understanding of the swelling behavior of UMo/Al fuel, some models with codes have been developed to simulate its swelling behavior. In the United States, the thermal model within PLATE was developed by Hayes et al. [16–18]. The thermal model within PLATE is based on a steady-state, three-dimensional, control-volume-based finite-difference

☆ Work supported by National Natural Science Foundation of China (grant no.11005094) and the Science Foundation of China Academy of Engineering Physics (grant no. 2010B0103007).

* Corresponding author at: Physics Department of Sichuan University, Key Laboratory for Radiation Physics and Technology of the Education Ministry, Chengdu 610064, PR China. Tel.: +86 8162495416; fax: +86 8162484280.
E-mail address: liuxiao6161@163.com (L. Xiao).

0925-8388/$ – see front matter © 2011 Elsevier B.V. All rights reserved.
doi:10.1016/j.jallcom.2011.03.099

temperature calculation implemented within a FORTRAN computer code. As the reaction-product phase increases and the matrix phase depletes, the effective fuel–meat thermal conductivity is continually modified through the use of an analytical multiphase conductivity model. In Europe, the French Atomic Energy Commission (CEA), in close collaboration with ANL, has developed a 2D thermo-mechanical code, called MAIA, to model the behavior of U-Mo dispersion fuel [19]. MAIA uses a finite-element method to resolve thermal and mechanical problems. The physical models (UMo/Al interaction-layer growth, fission-product swelling) are the same as those used in the ANL code, PLATE. The thermal properties of the meat are homogenized. These models usually include the fission-product swelling and interaction reaction between the fuel particle and matrix material; however, fission-product swelling in the UMo fuel alloy was calculated using an empirical equation developed from post-irradiation examination of UMo fuel plates. Fuel swelling by fission products is now considered the predominant factor. In this paper, we describe the primary physical models that are the basis of the FPIS (fission-product-induced swelling) mechanistic computer model for calculating fission-product-induced swelling of aluminum-dispersion fuels. Matrix-irradiation creep was also applied to the model to analyze the swelling behavior. In addition, we compare the calculated results with the values in the literatures. The theory of noble-gas behavior and its effect on fuel swelling is discussed. The behavior of fission products in the presence of irradiation-induced grain subdivision is presented. Models are also included for the effects of IL and of fabrication voids.

2. Theoretical mechanisms for the swelling by fission products

When uranium fission releases energy, medium-mass nuclei are produced. During irradiation, fuel plates increase in thickness because of swelling of the fuel core. The swelling is a direct result of the accumulation of fission-product elements in the fuel. Although this accumulation is, to first-order, directly proportional to the burn-up of the fissionable uranium, the resultant swelling is also affected by several microstructural changes that occur in the fuel core during irradiation. The fuel swelling is composed of two components: solid fission products and gaseous fission products. The solid swelling is proportional only to burn-up; it is independent of temperature and alloying conditions. The solid swelling is a linear function of burn-up:

$$\left(\frac{\Delta V}{V}\right)_s = 0.5\%\,\beta \tag{1}$$

where $(\Delta V/V)_s$ is the percentage of solid swelling and β is the burn-up.

The noble gases are not soluble in the fuel matrix, so the fuel swelling is a nonlinear function of burn-up for the gaseous fission products and is influenced not only by irradiation conditions but also by the initial fabrication technique. The noble-gas behavior is complex in fuel meat; however, the fuel swelling can be predicted by analyzing the diffusion of the fission gas atoms and the motion of the bubbles for given irradiation conditions and fabrication technique. Under irradiation, the total yield of fission gases, i.e., Xe and Kr, is

$$M = Y_g f t \tag{2}$$

where M is the yield of fission gases, Y_g is ~0.25 per fission, f is the fission rate and t is the irradiation time.

During irradiation, the release of the fission gases is either to external surfaces, such as the central void, cracks in the fuel, or the fuel-cladding gap, or to internal surfaces, such as grain boundaries. When the bubbles on the grain boundaries become sufficiently large and numerous, they can link together and release gas to one of the external surfaces. Nucleation of the gas bubbles is either homogeneous by chance encounter of wandering gas atoms or heterogeneous by fission-fragment tracks or dislocation lines. Fission-gas bubbles can act as very efficient traps for the atomically dispersed fission-gas atoms. Once nucleated, the bubbles are thought to simply grow in place by absorbing all the xenon and krypton produced by fission. Migration of the bubbles is either a random-walk process in the absence of direct forces acting on the bubble or a biased motion when such forces are present. The forces that act on gas bubbles in solids are generally believed to be caused by temperature or stress gradients or restraining forces due to dislocations and grain boundaries. The forced return of fission-gas atoms present in the bubbles in fuel into the matrix by irradiation is called re-solution. Re-solution can alleviate swelling and enhance gas release by several mechanisms, including the diffusion of gas atoms from the solid to surfaces from which escape is possible. The behavior of gaseous atoms and bubbles in the fuel can be calculated by coupled equations. Considering the above phenomena in which single-atom absorption by bubbles and re-solution occurring simultaneously with coalescence, the bubble conservation equation is given by a combination of Eqs. (3) and (4) [20],

$$\frac{dC_m}{dt} = k^{abs}_{1,m-1}C_1C_{m-1} - k^{abs}_{1m}C_1C_m - b_mC_m + \frac{1}{2}\sum_{j=2}^{m-1}\left(1+\delta_{j\frac{m}{2}}\right)k^{coal}_{m-j,j}C_{m-j}C_j - \sum_{j=2}^{\infty}(1+\delta_{jm})k^{coal}_{mj}C_mC_j \tag{3}$$

$$Y_g f t = C_1 + \sum_{m=2}^{\infty} mC_m \tag{4}$$

where $k^{abs}_{1,m}$ is the rate constant for single-atom absorption by a bubble of m atoms, $k^{coal}_{m,j}$ is the coalescence rate constant, b is the probability per unit time that an atom is redissolved, C_1 is the concentration of single gaseous atoms, C_m is the concentration of m gaseous atoms and mC_m is the total number of gaseous atoms contained in m-sized clusters in a unit volume. Eqs. (3) and (4) assume that a cluster of two gaseous atoms migrates as a bubble. From the coupled equations above, the bubble size distribution can be calculated by an iterative method.

UMo swelling has two distinct rates: a slow rate at low burn-up and a much faster rate at high burn-up. The phenomenon underlying the transition is the grain refinement or "grain subdivision" of UMo. After this transition, gas-bubble agglomeration accelerates [21]. The observation in UMo/Al that gas-bubble swelling depends on the burn-up has led to a theoretical formulation wherein the fission-induced stored energy in the material is concentrated on a network of grain-subdivision nuclei. This concentration diminishes with dose because of the interaction with radiation-produced defects. Grain subdivision starts when the energy per nucleus is high enough to offset the creation of grain boundary surfaces by creating strain-free volumes with a resultant net decrease in the free energy of the material [22].

During irradiation, UMo reacts exothermally with aluminum to form the reaction product UAl_x. Below the melting temperature, the reaction is diffusion-controlled and proceeds quite slowly. Irradiation enhances the diffusion rates [23]. In the UMo/Al system, temperature is an important consideration in determining the porosity and the formation of the reaction layer because it strongly influences the reaction rate between the fuel and the matrix. As the IL grows, the fuel temperature increases because its thermal conductivity is poorer than that of the aluminum matrix. Because IL has a lower density than the rest of microconstitutive, its growth

Table 1
The parameters of the $U_{10}Mo$/Al-dispersion fuel from the literature.

No.	Test	Plate ID	f (10^{20} m^{-3} s^{-1})	F (10^{27} m^{-3})	T (K)	V_f (%)	$\Delta V/V$ (%)	Reference
1	RERTR-3	V03	6.3	2.6	469	51.9	27.6	[26]
2	RERTR-2	V003	2.5	5	338	28.3	31.8	[26,27]
3	RERTR-2	A005	2.4	4.9	338	33	30.3	[21,27]
4	RERTR-5	V6018G	2.3	2.3	394	39.3	22.9	[21,28]
5	RERTR-5	V6019G	3.3	3.3	415	39.3	38.2	[21,28]
6	RERTR-5	V8005B	2.5	2.5	443	52.1	23	[21,28]

produces volume expansion of the fuel meat. Fuel–aluminum interaction is a contributor to meat swelling. The interaction depth y fits an irradiation-enhanced diffusion correlation developed with irradiation data from the literature [17]:

$$y^2 = 5.57 \times 10^{-23}(1.625 - 6.25 \cdot W_{Mo}) \exp\left(\frac{-10,000}{RT}\right) \cdot ft \qquad (5)$$

where y is the fuel–matrix interaction thickness, W_{Mo} is the weight fraction of Mo in the fuel, t is the irradiation time, R is the gas constant, and T is the temperature.

An important factor in reducing the net swelling is the radiation-enhanced sintering of fabrication voids. The fabrication voids within the UMo particles, as well as cracks and gaps resulting from fabrication, are sintered to spherical cavities after irradiation. It is well established that an increase in the dispersant loading also increases the number of fabrication voids. Inasmuch as a substantial fraction of the sintered porosity can be taken up by the swelling fuel, a large volume of fabrication voids can substantially reduce the net swelling.

3. Model of fission product-induced swelling

A model for the prediction of fission-product-induced swelling in aluminum-dispersion fuels has been applied to the analysis of UMo/Al-dispersion fuel swelling. The model calculates the irradiation-induced swelling of solid fission products and of fission gas bubbles as a function of fuel morphology. A system of spherical fuel particles is surrounded by a large spherical shell of matrix material bonded to an outer shell of aluminum cladding. The approach treats the inner sphere as a mechanically deforming body and the spherical shell as plastic. During irradiation, fission induces elastic deformation of the fuel particles. First, the fabrication pores in the matrix material close in response to the expansion of the fuel-particle volume. Next, the matrix materials creep, and plastic flow/swelling of the aluminum occurs. The subsequent macroscopic change in volume is caused by deformation processes. The mechanics relationship between the fuel particles and matrix is given by Eq. (6) [24]:

$$\sigma = \frac{rP}{2\delta} \qquad (6)$$

P is the gas pressure, r is the surface tension of the solid (r = 0.6 Jm^{-2}), σ is the radial component of the stress tensor at the fuel particle surface, and δ is the aluminum–matrix cladding thickness.

The fuel particles distribute randomly in the fuel matrix. The configuration relationship for the fuel plate element can be represented by

$$\delta = \left[\left(\frac{\pi}{6V_f}\right)^{\frac{1}{3}} - 1\right]\frac{d}{2} \qquad (7)$$

where d is the fuel-particle diameter and V_f is the fuel volume fraction.

The thermodynamic state of noble gases in the bubbles is most commonly described by the Van der Waals equation, which can be written as: [25]

$$P\left(\frac{1}{\rho_g} - B\right) = kT \qquad (8)$$

where P is the pressure of a gas of molecular density ρ_g at temperature T and k is the Boltzmann constant. The constant B expresses the volume occupied by the atoms.

During irradiation, the matrix material creeps. Two types of irradiation creep have been identified. The first is a transient creep due to the climb of pinned segments of the dislocation network in the solid, and the second is a steady-state form of creep arising from the collapse of vacancy loops. The creep rate can be represented by [24]

$$\frac{d\varepsilon}{dt} = K_c\sigma^3 e^{(-E_c)/(RT)} e^{\alpha F} \qquad (9)$$

where K_c is the creep constant ($K_c = 6.5 \times 10^{-30}$ Pa^{-3} s^{-1}), E_c is the creep activated energy (E_c = 9900 J mole^{-1}), and α is the irradiation-enhanced factor ($\alpha = 5 \times 10^{-29}$ m^3).

The following equation represents the total fuel swelling by fission products:

$$\left(\frac{\Delta V}{V}\right)_{total} = \left(\frac{\Delta V}{V_0}\right)_g + \left(\frac{\Delta V}{V_0}\right)_s - \left(\frac{\Delta V}{V_0}\right)_P \qquad (10)$$

The terms on the right-hand side of the equation represent the following sources of swelling, from left to right: gaseous products, solid fission products, and fabrication porosity. The subscript "0" on V denotes the initial volume.

The swelling models provide the driving force for mechanical deformation. In the model, the boundary conditions assume finite radial stresses at the center of the inner sphere and no discontinuity in the radial stress at the fuel/matrix interface. It is also assumed that the swelling is not a function of radial position.

The FPIS mechanical model calculates the plate behavior. During closure of fabrication porosity, the fuel-particle swelling is accommodated through the relatively soft aluminum matrix flowing into the existing porosity. During irradiation, fission-induced elastic deformation of the fuel particles occurs. The fabrication pores in the matrix material close in response to the expansion of fuel particle volume, the matrix materials creep, and plastic flow/swelling of the aluminum occurs. This model calculates the subsequent macroscopic changes in volume caused by fuel deformation processes.

4. Results and discussion

The behavior of the UMo/Al-dispersion fuel swelling was simulated using the above theory and model. The results were compared with the swelling data, and the good agreement indicates that this model is a plausible interpretation of the phenomenon. The values of the key parameters used in the model are given in Table 1. The irradiation data for the $U_{10}Mo$/Al fuel are summarized. Many of them are known or estimated from the literature [21,26–28]. V03 and V003 are from the RERTR-3 and RERTR-2 tests. The thick-

Table 2
Physical parameters used in the analysis.

No.	f (10^{20} m^{-3} s^{-1})	F (10^{27} m^{-3})	T (K)	V_f (%)	V_p (%)
S1	2.5	5.5	338	28.3	5
S2	2.5	5.5	394	28.3	5
S3	2.5	5.5	469	28.3	5
S4	2.5	5.5	394	39.3	5
S5	2.5	3.1	394	52.1	5
S6	1.5	5.5	394	39.3	5
S7	3.5	5.5	394	39.3	5
S8	2.5	5.5	394	39.3	10
S9	2.5	5.5	394	39.3	15

For S1–S3, the range of burn-up (F), fission rate (f), fuel volume fraction (V_f) and fabrication porosity (V_p) are the same; however, the temperatures are different. For S2, S4 and S5, the range of burn-up (F), fission rate (f), the temperatures (T), and fabrication porosity (V_p) are similar; however, the fuel volume fractions (V_f) are different. For S4, S8 and S9, the range of burn-up (F), fission rate (f), the temperature (T), and fuel volume fraction (V_f) are the same; however, the fabrication porosities (V_p) are different. For S4, S6 and S7, the range of burn-up (F), the temperature (T), the fuel volume fraction (V_f) and fabrication porosity (V_p) are the same; however, the fission rates (f) are different.

ness measurement taken outside of the fuel zone was subtracted from the average post-irradiation thickness measurements inside the fuel zone to determine an average plate-thickness change. The entire thickness change was assigned to the fuel meat swelling, and fractional swelling was calculated based on nominal fabrication meat thickness. A005 is from the RERTR-2 test. The actual particle size distribution was measured for a U-10Mo atomized fuel plate using the Johnson–Saltykov diameter method to normalize data from a fabrication fuel plate section. V6018G, V6019G and V8005B are from the RERTR-5 test. The meat-swelling data of fuel plates were gathered at various axial positions to obtain the overall thickness measurement. For these data, the irradiation conditions (f, F, T) and fabrication parameters (V_p, V_f) are different. To analyze the swelling behavior of the UMo/Al-dispersion fuel directly, the relationship between the physical parameters and the fuel-particle swelling was simulated by FPIS.

Table 2 describes the physical parameters used in the analysis. This database consists of S1–S9, which represent different irradiation conditions and fabrication parameters of U10Mo/Al-dispersion fuel. From Table 2, the range of burn-up is from 0 to 5.5×10^{27} m^{-3}, the fission rate is from 2.3 to 6.3×10^{20} m^{-3} s^{-1}, the temperature is from 338 to 469 K, the fuel volume fraction is from 28.3% to 52.1% and the fabrication porosity is from 5% to 15%. Results of the FPIS calculations are shown in Figs. 1–4.

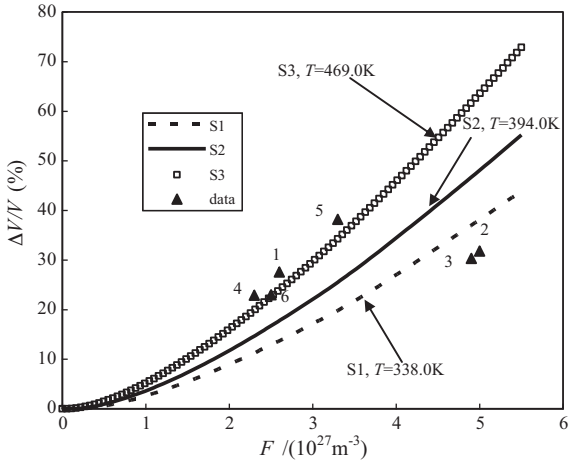

Fig. 1. FPIS-calculated fuel-particle swelling of U_{10}Mo/Al-dispersion fuel at three fuel temperatures. 1–6 denote irradiation data. S1–S3 denote the FPIS-calculated curves, and the input parameters are shown in Table 2.

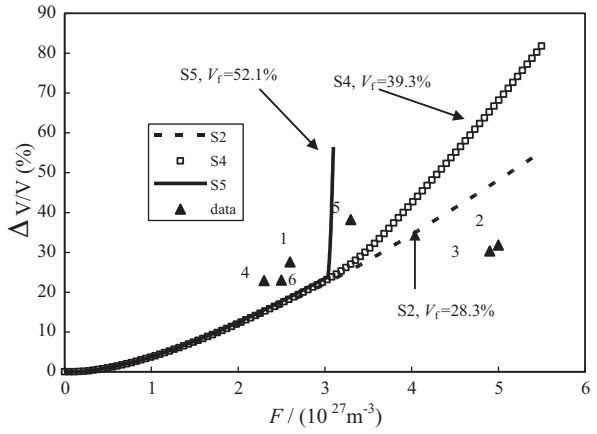

Fig. 2. FPIS-calculated fuel-particle swelling of U_{10}Mo/Al-dispersion fuel at three fuel-volume fractions. 1–6 denote the irradiation data. S2, S4 and S5 denote the FPIS-calculated curves, and the input parameters are shown in Table 2.

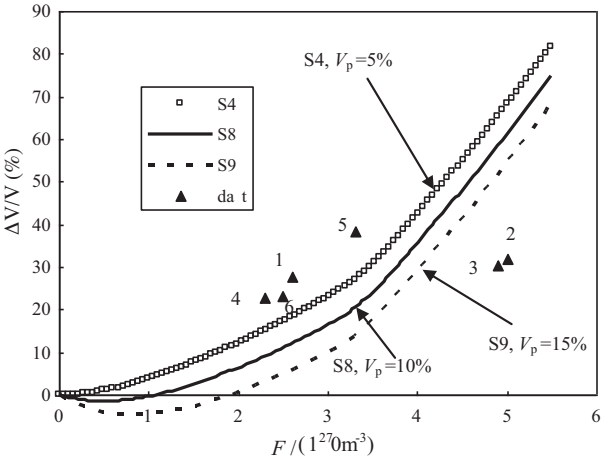

Fig. 3. FPIS-calculated fuel-particle swelling of U_{10}Mo/Al-dispersion fuel at three porosities. 1–6 denote the irradiation data. S4, S8 and S9 denote the FPIS-calculated curves, and the input parameters are shown in Table 2.

Fig. 1 shows the results of the FPIS-calculated fuel particle swelling of U_{10}Mo/Al-dispersion fuel containing 5% fabrication porosity for three different fuel temperatures. It is clear that the swelling of fuel is faster at higher temperatures. Many factors may lead to this result. First, the growth of interaction layer is strongly

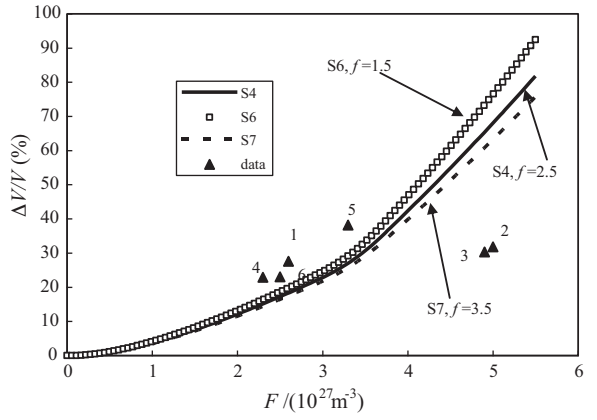

Fig. 4. FPIS-calculated fuel-particle swelling of U_{10}Mo/Al-dispersion fuel at three fission rates. 1–6 denote the irradiation data. S4, S6 and S7 denote the FPIS-calculated curves, and the input parameters are shown in Table 2.

dependent on the temperature; the square of the interaction layer growth is an exponential function of temperature, as shown in Eq. (5). When the temperature increases, the interfacial reaction will become faster. Second, as described in Eq. (9), when the temperature increases, the matrix-material creep accelerates. Finally, for a constant fission rate, the bubble pressure increases with increasing temperature, and therefore more fuel deformation occurs. All of these factors will lead to more significant fuel swelling at elevated temperature.

The calculated fuel particle swelling of $U_{10}Mo/Al$ containing 5% fabrication porosity for three values of fuel volume fraction is shown in Fig. 2. At low burn-up, the fuel swelling appears to be a function of the fission density, possibly with a short incubation period. The lines show the fuel swelling is faster at higher volumes in high burn-up conditions. The calculated values shown in Fig. 2 indicate that irradiation induces grain subdivision. Grain subdivision is predicted to occur earlier for irradiation at higher fuel volume fractions. From the S5 curve, we can see that the fuel swelling sharply increases after grain subdivision when the fuel volume fraction is higher than 52%. The results also indicate that the fuel swelling is faster at higher fuel volume fractions. As the fuel volume fraction increases, the thickness of the fuel particle shell will decrease, resulting in a decreased restraint imposed by the matrix material. This phenomenon may be the reason why the fuel swelling is faster at higher fuel volumes.

Fig. 3 shows the fuel-particle swelling of the $U_{10}Mo/Al$ dispersion as a function of the fission density at different fabrication porosities. Clearly, fabrication voids can reduce the net swelling.

The results of FPIS calculations of fuel-particle swelling on $U_{10}Mo/Al$ containing 5% fabrication porosity as a function of fission density at different fission rates at 394 K are shown in Fig. 4. The fuel swelling increased with increasing burn-up. Before the grain subdivision, the fuel swelling rates are nearly same. After the grain subdivision, the fuel swelling at lower fission rate is faster than that at higher fission rate. This phenomenon can be explained as follows. Before the grain subdivision, a majority of fission gases exist in the fuel in the form of single gaseous atoms. After the grain subdivision, most fission gases exist in the fuel with larger bubbles, which have a larger contribution to the fuel swelling. The possibility of larger bubbles increases with the irradiation time in the fuel, and the larger bubbles grow with sufficient time at lower fission for the same burn-up.

Figs. 1–4 depict the fuel-particle swelling of the UMo/Al-dispersion fuel as a function of fission density under different irradiation and fabrication parameters. The experimental conditions of datum 2 and datum 3 are similar to S1 and are thus near the S1 curve. Similarly, experimental points 4 and 5 are near the S4 curve and 1 and 6 are near the S5 curve. These results indicate that the model is consistent with the irradiation experience; however, there is deviation between simulation data and experimental data. The deviation may be explained as follows.

The FPIS model includes several assumptions. Among these is the assumption that no swelling of the aluminum matrix occurs during the reactor operation. This assumption is based on the relative swelling rates of the aluminum matrix and the fuel. The fuel particles are assumed to be identical in size and have a uniform spherical shape. The size of actual fuel particles varies, and their shapes are irregular. However, irregular particle shapes are difficult to handle mathematically, and because the orientation of the particles is random, an assumption of uniform overall behavior seems reasonable. In addition, particle–particle interactions are ignored. In addition to the uncertainties involving the model assumptions, various uncertainties exist in the experimental data. Physical measurements are subject to errors. The measurements are made at various points on the plate to yield an overall thickness and diameter measurement result in an average, which is subject to error. Measurement of the fabrication porosity is subject to uncertainties. Likewise, it is difficult to accurately measure matrix dimensions after fabrication. Actual interface conditions between both the fuel particles and the matrix and between the matrix and the cladding are not precisely known. All of these uncertainties will contribute to deviations between the model predictions and experimental data.

As is evident in Figs. 1–4, FPIS-calculated swelling of UMo/Al is in reasonable agreement with the experimental data in Table 1. The above analysis provides a plausible interpretation of the behavior of UMo/Al-dispersion fuel swelling.

5. Conclusion

The behavior of UMo/Al-dispersion fuel swelling is complex; however, it can be predicted by the fission-product-induced swelling. Although this analysis is far from rigorous, it does allow the following conclusions to be made.

(1) The motion of fission gas atoms, bubble growth and evolution and the creep of the matrix material are the basic behaviors of UMo/Al-dispersion fuel swelling. (2) The matrix-material creep will be accelerated at high temperature. (3) If fuel volume fraction is higher than 52%, the fuel swelling will sharply increase after grain subdivision. (4) Fabrication voids can reduce the net swelling. (5) Before the grain subdivision, the degrees of fuel swelling at different fission rates are not evidently different. After the grain subdivision, the fuel swelling at lower fission rates is faster than that at higher fission rates.

References

[1] D.E. Burkes, T. Hartmann, R. Prabhakaran, J.-F. Jue, J. Alloys. Compd. 479 (2009) 140–147.
[2] V.P. Sinha, G.J. Prasad, P.V. Hegde, R. Keswani, C.B. Basak, S. Pal, G.P. Mishra, J. Alloys. Compd. 473 (2009) 238–244.
[3] A. Daoudi, M. Potel, H. Noel, J. Alloys. Compd. 232 (1996) 180–185.
[4] D.B. Lee, K.H. Kim, C.K. Kim, J. Nucl. Mater. 250 (1997) 79–82.
[5] K.-H. Kim, J.-M. Park, C.-K. Kim, G.L. Hofman, M.K. Meyer, Nucl. Eng. Des. 211 (2002) 229–235.
[6] H. Palancher, N. Wieschalla, P. Martin, R. Tucoulou, C. Sabathier, W. Petry, J.-F. Berar, C. Valot, S. Dubois, J. Nucl. Mater. 385 (2009) 449–455.
[7] D.D. Keiser, B. Yao, E. Perez, Y.H. Sohn, 2009 International meeting on RERTR, Beijing, China, 2009.
[8] M.I. Mirandou, S.F. Aricó, S.N. Balart, L.M. Gribaudo, Mater. Charact. 60 (2009) 888–893.
[9] J. Gan, D.D. Keiser, D.D. Miller, M.A. Kirk, J. Rest, T.R. Allen, D.M. Wachs, J. Nucl. Mater. 407 (2010) 48–54.
[10] Y.S Kim, G.L Hoffman, 2009 International meeting on RRFM, Vienna, 2009, pp. 143–148.
[11] J.L. Snelgrove, P. Lemoine, L. Alvarez, 2005 International meeting on RRFM, Budapest, 2005, pp. 64–72.
[12] M. Ugajin, A. Itoh, M. Akabori, N. Ooka, Y. Nakakura, J. Nucl. Mater. 254 (1998) 78–83.
[13] M.K. Meyer, G.L. Hofman, T.C. Wiencek, S.L. Hayes, J.L. Snelgrove, J. Nucl. Mater. 299 (2001) 175–179.
[14] M. Cornen, M. Rodier, X. Iltis, et al., 2008 International meeting on RRFM, Hamburg, 2008, pp. 111–116.
[15] C. Jarousse, L. Halle, W. Petry, et al., 2009 International meeting on RRFM, Vienna, 2009, pp. 15–22.
[16] S.L. Hayes, G.L. Hofman, M.K. Meyer, J. Rest, J.L. Snelgrove, 2002 International meeting on RERTR, San Carlos de Bariloche, Argentina, 2002.
[17] D.M. Wachs, D.E. Burkes, W. Skerjanc, et al., 2006 International meeting on RERTR, Southern Sun Cape Sun, Cape Town, Republic of South Africa, 2006.
[18] Y.S. Kim, G.L. Hofman, P.G. Medvedev, et al., 2007 International meeting on RERTR, Czech Republic, 2007.
[19] V. Marelle, F. Huet, P. Lemoine, 2004 International meeting on RRFM, München, Germany, 2004, pp. 188–192.
[20] J.-n. Yu., The Irradiation Effect of Material, Beijing, 2007 (in Chinese).
[21] J. Rest, G.L. Hofman, Y.S. Kim, J. Nucl. Mater. 385 (2009) 563–571.
[22] J. Rest, G.L. Hofman, J. Nucl. Mater. 223 (1995) 192–195.
[23] A. Savchenko, A. Vatulin, I. Dobrikova, Y. Konovalov, 2006 International meeting on RRFM, Sofia, 2006, pp. 121–125.
[24] Z.-h. Xing, S.-h. Ying, Atomic Energy Science and Technology, vol. 35, 2001, pp. 15–19 (in Chinese).

[25] D. Olander, Fundamental Aspects of Nuclear Reactor Fuel Elements, Technical Information Center, Office of Public Affairs, U.S. Energy Research and Development Administration, New York, 1976.
[26] M.K. Meyer, G.L. Hofman, et al., 2000 International meeting on RERTR, Las Vegas, 2000.
[27] M.K. Meyer, G.L. Hofman, J.L. Snelgrove, et al., 1999 International meeting on RERTR, Budapest, 1999.
[28] G.L. Hofman, M.R. Finlay, Y.S. Kim, 2004 International meeting on RERTR, Vienna, 2004.